Published in final edited form as:
J Immunol. 2013 March 1; 190(5): 2090–2101. doi:10.4049/jimmunol.1202810.

Studies of lymphocyte reconstitution in a humanized mouse model reveal a requirement of T cells for human B cell maturation

Julie Lang[*], **Margot Kelly**[*], **Brian M. Freed**[†], **Martin D. McCarter**[‡], **Ross M. Kedl**[*], **Raul M. Torres**[*], and **Roberta Pelanda**[*]

[*]Integrated Department of Immunology, National Jewish Health and University of Colorado Denver School of Medicine, Denver, CO 80206, USA

[†]Division of Allergy and Clinical Immunology, University of Colorado Denver School of Medicine, Aurora, CO 80045, USA

[‡]Department of Surgery, University of Colorado Denver School of Medicine, Aurora, CO 80045, USA

Abstract

The hematopoietic humanized mouse (hu-mouse) model is a powerful resource to study and manipulate the human immune system. However, a major and recurrent issue with this model has been the poor maturation of B cells that fail to progress beyond the transitional B cell stage. Interestingly, a similar problem has been reported in transplant patients that receive cord blood stem cells. In this study, we characterize the development of human B and T cells in the lymph nodes (LNs) and spleen of BALB/c-Rag2^{null}Il2rγ^{null} hu-mice. We find a dominant population of immature B cells in the blood and spleen early, followed by a population of human T cells, coincident with the detection of LNs. Notably, in older mice we observe a major population of mature B cells in LNs and in the spleens of mice with higher T cell frequencies. Moreover, we demonstrate that the T cells are necessary for B cell maturation, as introduction of autologous human T cells expedites the appearance of mature B cells, while *in vivo* depletion of T cells retards B cell maturation. The presence of the mature B cell population correlates with enhanced IgG and Ag-specific responses to both T-dependent and T-independent challenges, indicating their functionality. These findings enhance our understanding of human B cell development, provide increased details of the reconstitution dynamics of hu-mice, and validates the use of this animal model to study mechanisms and treatments for the similar delay of functional B cells associated with cord blood transplantations.

Introduction

The hematopoietic humanized mouse, in which human hematopoietic stem cells (HSCs) drive the development of a human hematopoietic system within a mouse host, provides a unique *in vivo* model to perform mechanistic, genetic and pharmacological studies of the human immune system. Current host models enable notable human engraftment due to a lack of T, B and NK cells as a result of null genetic mutations in the *Il2rγ* and either *Rag* or *Prkdc* genes (1–6). The genetic background of the mouse strain is an important factor in

Address correspondence and reprint requests to Roberta Pelanda, Ph.D., National Jewish Health, Integrated Department of Immunology, 1400 Jackson St. Rm K814a, Denver, CO 80206; pelandar@njhealth.org; ph: 303-398-1451; fax: 303-270-2325.

Disclosures
The authors declare no competing financial interests.

human engraftment and multi-lineage engraftment has been demonstrated in both the NOD and the BALB/c mutant strains (1–8). However, the frequencies of distinct hematopoietic lineages in hu-mice differ from those in a human.

In the bone marrow (BM) of hu-mice, human HSCs differentiate into pro-B, pre-B and immature B cells, suggesting that the mouse environment supports human B cell development (9–13). However, several studies have shown that human B cells are blocked in maturation at the transitional stage in the PBL and spleen: the majority of hu-mice are populated primarily with immature B cells (14–17) that are inferior to mature B-cells in their ability to respond to Ag (18). Not surprisingly, immunization challenges have yielded only weak immune responses in hu-mice compared to those achieved in immunologically intact mice or humans (1, 2, 10, 14–16, 19). A major goal in the hu-mouse field is the generation of a high-affinity, mutated Ab response to antigenic challenge (20). One obvious requirement is the generation of a mature B cell population.

The transplantation of CB HSCs now account for more than 25% of all hematopoietic transplantations in humans due to enhanced availability and a lower requirement for HLA-matching compared to BM. However, infection-associated mortality resulting from a delayed reconstitution of the human immune system following CB transplantation remains a current challenge in the field (21). Specifically, B cells are found to re-populate the recipient early after engraftment, yet have limited functionality for up to six months, around the time when significant T cell reconstitution occurs. Thus, reconstitution of functional B cells appears to be limited not only in hu-mice but also in human CB recipients. Therefore, the hu-mouse has the potential to be a useful animal model to investigate and solve issues related to CB transplantation.

Unlike typical mouse BM chimeras, hu-mice have a dynamic and inconsistent engraftment of hematopoietic lineages over time (1, 4, 22). Thus, understanding the details of human lymphocyte reconstitution in the primary and secondary organs and the factors that shape the B cell population is vital for appropriate experimental design using this model. In this study, we characterize the frequency, maturation, and activation patterns of human T and B-lymphocytes in the BM, spleen, PBL and LNs of BALB/c-Rag2^{null}Il2rγ^{null} (BALB/c-DKO) hu-mice generated with a protocol that we have optimized to reproducibly promote high levels of human chimerism (23). More importantly, we define the kinetics and reconstitution pattern of mature B cells in these hu-mice and report a requirement of T cells for human B cell maturation. Furthermore, we compare the tissue organization of T and B cells and the immune responses to T cell dependent (TD) and independent (TI) Ags in hu-mice with mature B cells to those with mostly immature B cells. Our study not only provides a detailed characterization of lymphocytes in hu-mice but also insights into mechanisms of human B cell maturation. We propose that the hu-mouse is an informative *in vivo* model that can be used to study factors necessary for human lymphocyte development and function.

Materials and Methods

CD34$^+$ and CD34$^-$ cell preparation from human umbilical CB

Human cell preparation was performed as described previously (23). CB mononuclear cells were isolated over Ficoll-density gradients and CD34$^+$ cells were enriched using AutoMACS (Miltenyi Biotech) technology. The CD34$^-$ cell fraction was further depleted of T cells with CD2 and CD3 specific beads and used immediately or frozen for later use as "support" cells. The CD34$^+$ cells were used immediately or cultured at 1×10^5 cells/ml in IMDM supplemented with 10% FBS, 50 μM 2-ME, 2 mM Glutamax, IL-6 (10 ng/ml), stem cell factor (20 ng/ml), and FLT3 (10 ng/ml). Cultured CD34$^+$ cells were harvested 1 to 7

days later and either used immediately or frozen in FBS and 10% DMSO at −80°C for future use.

Mice and hematopoietic stem cell transplantation

BALB/c-Rag2^{null}Il2rγ^{null} (BALB/c-DKO) mice were bred and maintained on a diet enriched with Septra every other week, under specific pathogen-free and BSL2 conditions at the Biological Resource Center at National Jewish Health (NJH). Animal care and experiments were approved by the NJH Institutional Animal Care and Use Committee. For HSC transplantation, CD34$^+$ enriched cells (~1×10^5 CD34$^+$ cells/mouse) and T cell-depleted CD34$^-$ "support" cells (4–15×10^5 cells/mouse) were resuspended together in sterile PBS. Newborn BALB/c-DKO mice (1–3 d old) were irradiated with 350 rad using a Cs-137 gamma irradiator. The pups were injected 4-to-6 h after irradiation with 50 μl of cell suspension using a 30 G needle into the facial vein and, when unsuccessful, into the liver (23).

Human and mouse single cell sample preparations

Human adult PBL samples were collected from healthy donors in the Clinical Division of NJH. Human spleen and LN samples were either collected from cadavers from the International Institute for the Advancement of Medicine or from individuals that underwent surgery at the University of Colorado Hospital. The human BM sample was obtained from Lonza. The studies were performed in compliance with the NJH and University of Colorado Denver Institutional Review Boards. Mouse PBL samples were collected either by submandibular or tail vein bleed and processed over a Ficoll-density gradient for leukocyte preparation. Serum was prepared by centrifugation of naturally clotted blood. Single cell suspensions of all tissues were prepared by standard methods, filtered over cotton plugs to remove aggregates and debris, and removal of erythrocytes with ACK lysis buffer (0.15 M NH_4Cl, 10 mM $KHCO_3$, 0.1 mM EDTA, pH 7.2). For mice in which LNs were not visible by naked eye, small tissue samples at LN sites were nevertheless processed for analysis.

Abs and flow cytometry

Abs used in FACS were against: hCD3 (clone UCHT1), hCD45 (H130), hCD10 (H10a), hCD24 (ML5), hCD22 (HIB22), hCD21 (LT21), hCD19 (HIB19), hCD20 (2H7), hCD45RB (MEM-55), hCD5 (UCHT2), hCD27 (323), hCD11c (3.9), hIgD (IA6-2), hCXCR4 (12G5), and hCXCR5 (TG2) from Biolegend; hCD4 (RPA-T4), hCD8 (RPA-T8), hCD20 (L27), hCD45RA (HI100), hCD45RO (UCHL1), hCD40 (5C3), hHLA-DR (G46-6), hCD268 (11C1), hCD70 (Ki-24), hCD25 (M-A251), hCD69 (FN50), hCD80 (L307.4), hCD11c (B-ly6), hCD95 (DX2), hIgM (G20-27), hIgD (IA6-2), hIgG (G18-145), hκ (G20-193), hλ (JDC-12), hCD44 (G44-26, BD), hLFA-1 (G43-25B, BD), hCD80 (L307.4, BD), hCD86 (2331), hCD197("CCR7," 3D12), hCD2 (RPA-2.10), hCD28 (CD28.2), hCD49d (9F10) and hCD34 (581) from BD Biosciences; hCD5 (UCHT2), mCD45 (30-F11), hCD38 (HT2), hCD21 (BU32), hCD23 (EBVC32), hIgM (SA-DA4), hCD62L (Dreg56), and hCD196 ("CCR6," R6H1) from E-Bioscience; and hCD122 (27302) from R&D systems. Biotinylated Abs were revealed with streptavidin fluorescent conjugates (Invitrogen). To distinguish dead cells, 7-AAD (BD) was added to some samples within 30 minutes of analysis. All cell samples were run on a Cyan analyzer (Beckman Coulter) and analyzed with FlowJo software (Tree Star). All flow cytometric analyses were based on a single cell gate based on forward and side-scatter and doublet discrimination.

Histology

Intact LN and spleen tissue samples were imbedded in Tissue-Tek® O.C.T. compound (Sakura Finetek), frozen immediately on dry ice and stored at −80°C. Frozen samples were

sliced into 4–7 μm thick sections on a cryostat and transferred onto glass slides. Slides were dried at room temperature overnight and either frozen or directly fixed for 10 min in 4% formaldehyde. Each section was rehydrated for 15 min in PBS followed by blocking for 15 min with avidin (Avidin/Biotin blocking kit, Vector Laboratories), and then for 15 min with a mixture of biotin, mouse IgG, human IgG, anti-mouse CD16 Abs (24G2), and goat serum. Tissue sections were stained with either anti-human CD20 (APC) and CD3 (PE) Abs or anti-human CD45 (APC) and anti-mouse CD45 (PacB) Abs for 1h. After three washes, dried sections were mounted with a coverslip using Fluoromount G (Southern Biotech) and sealed with nail polish. Sections were visualized on an Axiovert 200 M microscope (Carl Zeiss) outfitted with a 3i Marianas system and analyzed with SlideBook 4.0 software (Intelligent Imaging Innovations).

T cell adoptive transfer and T cell depletion

Human T cells were isolated from CB preparations upon positive selection with anti-CD2 beads (Miltenyi Biotech) at the time of $CD34^+$ cell purification and were frozen at −80°C until use. T cells were thawed, washed, resuspended in PBS and injected into the tail vein of 11–12 wk-old hu-mice (6×10^6 cells/mouse) that had been engrafted with HSC from the same CB prep. Control hu-mice were either left untreated or injected with a similar number of T cell-depleted $CD34^-$ CB cells. For T cell depletion, hu-mice were injected twice weekly with 10 μg of anti-CD3 Abs (UCHT1 or OKT3) starting at 9 wks of age. Control mice were left untreated. PBL were collected every 3–4 wks to assess human T and B cell chimerism. Hu-mice were euthanized for tissue collection and analysis when significant T cell chimerism was established in control untreated littermates (generally between 18 and 24 wks).

Immunizations

Hu-mice were separated into groups according to their level of human chimerism established by flow cytometric analyses of leukocytes in PBL at 7–8 wks of age. The mice were injected either i.p. or s.c. under the scruff of the neck with the following vaccines: NP-Ficoll (100 μg, Biosearch Technologies) or Diptheria, Tetanus, and Pertussis (DTaP, 50 μl, Sanofi Pasteur). All mice were inoculated every other wk for a total of 3–4 times beginning at 8–12 wks of age or 14–16 wks of age. No differences were observed between i.p. and s.c. immunizations.

ELISAs

Total human IgM and IgG concentrations were determined as described previously (23). During the optimization of Ag-specific ELISA, sera were collected from immunized (DTaP and NP-Ficoll) BALB/c-DKO hu-mice (“test” group); unimmunized hu-mice, non-humanized BALB/c-DKO and CB17 mice (negative controls); and human CB and PBL (positive controls) by standard methods. The hu-mice had serum Ig concentrations of 0–670 μg/ml (IgM) and 0–3200 μg/ml (IgG). We tested coating the plates with the following Ags, all diluted in PBS: Nicked DT (10 μg/ml, List Biological Laboratories), DTaP vaccine (1:333, Sanofi Pasteur), NP_{36}CGG (10 μg/ml) and NP_{16}CGG (10 μg/ml) along with a PBS-only plate. In addition, we tested blocking plates with PBS-1% BSA, 3% BSA, 20% FBS, or 1% gelatin; washing the plates with PBS-0.5% Tween-20, 0.1% Tween-20, or TBS 0.1% Brij solutions; diluting the serum in PBS-1% BSA or PBS-0.05% Tween-20; and detecting bound Igs with the following Abs conjugated to alkaline-phosphatase (AP): monoclonal mouse-, and polyclonal goat-, anti human IgM or IgG (Southern Biotech).

The ELISA protocol for measuring Ag-specific responses was adopted from optimization assays described above and limited to IgM samples with concentrations of 1–35 μg/ml to limit background effects. ELISA plates were coated overnight at 4°C with 10 μg/ml NP_{16}-

BSA or a 1:333 dilution of DTaP vaccine in PBS and duplicate plates were left uncoated (PBS) to measure background values. Plates were washed in PBS-0.1% Tween-20 and blocked with PBS-1%-BSA. Two-fold serial dilutions of sera starting at 1:10 or 1:20 in PBS-1%-BSA were incubated overnight at 4°C. Positive (human sera for DTaP) and negative (BALB/c-DKO sera) controls were added to most plates. The following day, plates were washed and incubated for 2–4 h at 37°C with AP-conjugated mouse anti-human (for NP) or goat anti-human (for DT) IgM or IgG Abs (Southern Biotech). After a final wash, the AP substrate p-nitrophenyl phosphate (Sigma-Aldrich) was added to plates and light absorbance was measured at OD_{405} on a Versamax microplate reader (Molecular Devices). Background values obtained from wells developed in the absence of sera and then values obtained from duplicate PBS-coated wells were subtracted from sample OD_{405} values. Relative Ab titers were defined as the serum dilution that generated an OD_{405} equal to 0.5 for NP and 0.25 for DT. Comparable responses of identical samples performed on different days were used to normalize the relative Ab titers. Data presented represent the average response of a serum measured 1–4 times.

Statistical Analysis

Statistical significance was assessed using Prism software (GraphPad Software) with a two-tailed Student's t-test of equal variance or Welch's correction when appropriate.

Results

Kinetics of human B cell, T cell, and LN development in BALB/c-DKO hu-mice

To define the engraftment kinetics in our BALB/c-DKO hu-mouse model, we used FACS analysis to measure the percentage of human hematopoietic ($hCD45^+$) cells in both primary (BM, thymus; Fig. 1A, left panel) and secondary (PBL, LN, and spleen; Fig. 1A, middle panel) lymphoid tissues of hu-mice over time. Similar to other reports (1, 3), human hematopoietic cell engraftment was observed as early as six wks, but steadily declined thereafter in the BM and PBL (Fig. 1A). Notably, we found that the human engraftment kinetics were unique to distinct lymphoid organs. Human chimerism was detected early in the thymus and was sustained over time (Fig. 1A, left panel). Conversely, splenic engraftment was delayed relative to BM, was maximal between wks 15–24 and then declined sharply, as human hematopoietic production in the BM waned (Fig. 1A). Unlike in the spleen or BM, mouse $CD45^+$ hematopoietic cells were rare in the LN or thymi in hu-mice, so that >90% of the hematopoietic cells, if present at all, were human in these tissues (data not shown). Engraftment in the LN was detected only in a fraction of hu-mice, which was a majority by 16 wks, and was not affected by immunization (Fig. 1B). Human cells were detected in mesenteric LNs prior to peripheral LNs, although in older mice, occupation of cervical, inguinal, axillary and iliac LNs by human cells was common, and the size of LNs in these hu-mice was comparable to that in wild-type mice (Fig. 1C). The absolute numbers of human cells roughly mirrored their frequencies, with consistent numbers over time in the thymus, a decrease in the spleen at later time points, and a delayed appearance in the LNs (Fig. 1A, right panel). Thus, an optimal window of human hematopoietic chimerism generally exists in both primary and secondary lymphoid organs between 15 and 24 wks of age (or post-transplantation), although this window can shift by several weeks in individual mice.

FACS analysis of human B cell (CD19, CD20) and T cell (CD3) subsets revealed a consistent pattern of early B lineage and delayed T lineage reconstitution (Fig. 1D), similar to murine and human HSC transplantation (24, 25). T and B cell ratios varied greatly over time in the PBL and spleen, but once established in the LNs they remained consistent for several weeks and were similar to LNs in humans and wild-type mice (~60% T, 20% B). In

a subset of mice, notably those examined at later time points (>24 wks), the human T cell engraftment represented the majority of the human cells (Fig. 1D). Although variability in the timing and amount of chimerism existed among individual HSC recipients, the pattern of early B cell and later T cell reconstitution was a consistent finding. In contrast to the frequency, the absolute number of human B cells in the spleen remained fairly constant, while the number of human T cells increased sharply (Fig. 1D, bottom panels). In the LNs, the number of human T and B-lymphocytes escalated between 10 and 20 wks of age (Fig. 1D). In all cases, LNs contained a majority of human T cells, suggesting B cells alone could not seed this tissue.

Both human IgM and IgG were present in the sera of hu-mice at increasing concentrations beginning at 9 wks post engraftment (Fig. 1E). Of note, concentrations of hIgG were higher than of hIgM, suggesting that many human B cells in hu-mice undergo Ig class switch. The presence of engrafted LNs in individual mice significantly correlated with serum Ig (Fig. 1F).

Mature B cells are present in all LNs and in the spleen of some hu-mice

Several studies have reported an immature phenotype of B cells in hu-mouse models, warranting skepticism about their use for B cell studies (14–16). We investigated the state of B cell maturation in our hu-mice by analyzing the expression of CD10, CD24 and CD38 that are high on immature and low on mature B cells. In agreement with other studies (14, 15), we found mostly immature B cells in the spleen and PBL of many chimeric mice (Fig. 2A and data not shown). However, we also observed a significant fraction of mature B cells in all LNs, and in the spleen of some hu-mice (Fig. 2A). These data were confirmed by additional analysis of the expression of CD21 and CD22 that are low on immature and high on mature B cells (data not shown).

Upon the analysis of 215 chimeras, we categorized hu-mice into the following five distinct phenotypes based on the presence or absence of LNs and the frequency of mature ($CD10^-$) B cells in the spleen: I) LN^-, <25% $CD10^-$; II) LN^+, <25% $CD10^-$; III) LN^-, >25% $CD10^-$; IV) LN^+, 25–60% $CD10^-$; and V) LN^+, >60% $CD10^-$. Figure 2A shows representative FACS analysis while Figure 2B reports the frequency of $CD10^-$ mature B cells in the spleen of hu-mice assigned to different categories, relative to BM and LN. We found that the percentage of hu-mice with LNs and mature B cells in the spleen increases substantially with age, representing a majority by 18 wks (Fig. 2C). Moreover, we observed a positive correlation between mature B cell development in the spleen and both total human leukocytes and T cell frequencies (Fig. 2D), with the exception of mice in category III that do not develop LNs but still harbor a high frequency of mature B cells in the spleen (Figs. 2B,D)

These observations suggest that the human hematopoietic system evolves with time in hu-mice and reaches conditions that foster the generation of mature B cells in most animals.

Characterization of B cells in hu-mice

To better understand the B cell populations that develop in hu-mice, we characterized the expression of multiple surface markers on B cells in the BM, LN and spleens of hu-mice displaying immature (categories I–II) or mature (categories III–V) B cells. We compared the expression of these proteins not only to B cells of human cord and adult blood, but also to those of human spleen, LN and BM since there might be tissue-specific differences in the B cell phenotype. These data are shown in Table I in which the markers are divided into distinct categories: B lineage (CD19, CD20, CD45RA, CD45), immature B cell (CD5, CD10, CD24, CD38), mature B cell (CD40, HLA-DR, CD21, CD22, CD268, CD23),

activation or memory (CD27, CD70, CD25, CD69, CD80, CD86, CD122, CD11c, CD95, CD45RB), Ig receptors (IgM, IgD, IgG), and chemokine or adhesion receptors (CD62L, CD44, CD49d, LFA-1, CCR6, CCR7, CXCR4, CXCR5). As shown previously, human B cells developing in the BM of hu-mice display characteristics very similar to B cells found in human BM (9, 15). Moreover, this analysis confirms that B cells in hu-mice of categories I and II are more immature than those of hu-mice classified as III–V. It also indicates that mature B cells of hu-mice are capable of activation and Ig class-switch as evident by the expression of CD27, CD11c, CD95, CD45RB and IgG. In most cases, mature B cells in the LN and spleen of hu-mice express proteins at similar levels as those observed on B cells from human controls, with the exception of CD268 (BAFF receptor), which is expressed on B cells of hu-mice at only 10–20% of control B cells (Table I).

Numbers and phenotype of T cells in hu-mice that harbor immature or mature B cells in the spleen

The analysis of human T cell frequencies and numbers in the spleen of hu-mice revealed a larger T cell population among mice with mature splenic B cells (Fig. 3A). This correlation was confirmed by a linear regression analysis displaying the percentage of mature B cells, defined as $CD10^{-}$ or $CD22^{+}$ (Fig. 3B), as a function of the T cell frequencies in the spleen. To extend these findings, we examined the expression of markers on T cells in peripheral organs of hu-mice to determine whether the presence of mature B cells correlated with a particular T cell phenotype. We found that LNs displayed a higher percentage of CD4 T cells compared to the spleen, but there was no distinct correlation of CD4 (and conversely CD8) T cells with B cell maturation in the spleen (Fig. 3C). In mice with immature or mature splenic B cells, clear differences were not observed in the expression of numerous T cell proteins including activation markers (CD69, CD25, CD44, CD62L and CD122; Fig. 3C and data not shown), homing receptors (CCR7, CXCR4, CXCR5, and LFA-1; data not shown) or signaling receptors (CD2, CD3, CD5, and CD27; data not shown). However, T cells expressing the memory marker CD45RO and the activation markers HLA-DR and CD49d were more frequent in LNs and spleen of hu-mice displaying mature B cells than in the spleen of hu-mice with immature B cells (Fig. 3C, lower panels). We also noticed a relatively large proportion of $7\text{-}AAD^{+}$ dying T cells in the LNs and spleen, but not in the BM, of hu-mice, but there was no correlation with the presence of mature B cells (Fig. 3C, upper right panel). These data suggest that T cells, and potentially their activation state, might be important for B cell maturation in hu-mice.

Improved Ab responses to TI and TD Ags in hu-mice with mature B cells

To evaluate whether increased numbers of mature B cells support higher Ig production, we measured over time the concentrations of hIgM and hIgG in sera of hu-mice classified into categories I–V. There was very little detectable IgM or IgG in mice with only immature B cells (Fig. 4A, category I), while the presence of mature B cells in either the LN or spleen (categories II–V) correlated with increased hIgM and hIgG (Fig. 4A).

The generation of a class-switched, Ag-specific Ab response upon immunization is currently a major challenge in the hu-mouse model. The predominant immature B cell population is considered partly responsible for this immunodeficiency (18). We reasoned that we should see improved Ag-specific responses in mice with mature B cells. To test this hypothesis, we immunized hu-mice with the TI-II Ag, NP-Ficoll, or the TD Ag, DTaP, and measured the respective Ab responses.

Initial observations indicated that the determination of Ag-specific responses in hu-mice is challenging due to the extreme variation of hIg levels among individual mice (Fig. 1F). Comparing responses among hu-mice is complicated by two major factors which both

correlate with sera Ig concentrations: 1) a nonspecific background that is measured in sera even from plates that are not coated with Ag, and 2) a polyreactive response to Ag, most notably of the IgM isotype, that is detected in sera of both unimmunized and immunized mice. To limit the effect of these issues on our analyses, we compared Ab-responses only in mice displaying a limited range of IgM concentration (1–35 μg/ml), and subtracted the background signal detected on plates in the absence of Ag from the signal measured in the Ag-coated plates for each sample.

No response was ever detected in sera from non-humanized BALB/c-DKO mice, or from hu-mice without detectable Ig, indicating that a background response measured in naïve hu-mice was due to Igs (Fig. 4B). Both the TI and TD Ag-specific Ab responses were increased in hu-mice that were immunized after 14 wks, when mature B cells are more prevalent (Fig. 4B). This increase was more pronounced for the IgM responses, although the IgG responses from mice immunized after 14 wks also showed modest increases over those mice that were unimmunized or immunized before 14 wks (Fig. 4B). Even in mice immunized early, the presence of mature B cells in some hu-mice resulted in DT-reactive Ab levels above the background observed in unimmunized hu-mice (Fig. 4B). Nevertheless, IgG responses to the TD Ag were weak even when vaccinated after 14 wks, suggesting that other factors in addition to B cell maturation are required for an optimal Ig class-switched Ab response.

Increased co-localization, yet abnormal organization, of mature B and T cells in hu-mice

In humans and mice, T and B-lymphocytes are organized into distinct zones within secondary lymphoid tissue. Previous histological analyses have shown a lack of organization of human T and B cells in spleens of hu-mice (8, 10, 26). We questioned whether lymphoid organization improves in LNs and spleen of hu-mice that develop mature B cells.

To address this question, we performed immunohistochemistry on spleen sections of hu-mice in categories I–II (immature B cells) and IV–V (mature B cells) and compared them to human spleen sections. LN tissue sections, in which the B cells are predominantly mature, were also analyzed. In most hu-mice with immature splenic B cells, the human and mouse hematopoietic cells were interspersed and randomly scattered throughout the spleen without any discernable organization (Fig. 5, I/II). Increased organization of human B cells into discrete follicle-like structures was only observed in the spleen of a category II hu-mouse that had a large B cell population (Fig. 5, SP II). In the LNs and spleens of mice with mature splenic B cells, human T and B cells co-localized, with some T cells also scattered outside these foci (Fig. 5, IV/V). However, none of the mice exhibited a T-B cellular organization similar to that seen in human spleens (Fig. 5) (27). Therefore, our data suggest that more T-B cell interactions likely occur in hu-mice with higher numbers of T cells and mature B cells, potentially supporting better immune responses despite abnormal lymphoid organization.

Requirement of T cells for B cell maturation in hu-mice

The correlation observed between the number of T cells and the presence of mature B cells in the spleen of hu-mice (Figs. 2D, 3A, and 3B) led us to hypothesize that T cells provide signals necessary for B cell maturation. To test this hypothesis, we performed experiments, in which we either added exogenous T cells (Fig. 6A) or depleted developing human T cells in hu-mice (Fig. 6B). Enumeration of T and B cell populations indicated that both T cell treatments were effective, as T cell numbers were higher in hu-mice adoptively transferred with T cells and lower in those with anti-CD3 treatments, while total B cell numbers were similar in all animals (Figs. 6A,B). The adoptive transfer of autologous T cells to hu-mice led to a significant increase in the frequency of $CD10^{-}$ and $CD22^{+}$ mature B cells in the spleen (Figs. 6A and S1A). In contrast, when human T cells were depleted with injections of

anti-CD3 Abs, the percentage of mature B cells was significantly reduced compared to control hu-mice (Figs. 6B and S1B). Thus, these data support our hypothesis that T cells are required for B cell maturation. In further support, a highly significant linear correlation was observed between the frequency of T cells and that of mature B cells in the spleen of these hu-mice (Fig. 6C). The effect of T cells was also clearly evident on LN development in these experiments, as only mice with significant T cells displayed obvious LNs that bore higher numbers of human lymphocytes (data not shown).

The results from these experiments indicate that human T cells play an important role in the generation of mature human B cells.

Discussion

This study provides a detailed description of human T and B lymphocyte engraftment in BALB/c-DKO hu-mice with an extensive characterization of these cells over time. Importantly, we show that human T and B cell engraftment is a dynamic, yet predictable, process. We observed that immature B cells dominate the human population early after engraftment, and that T cells appear wks later, coincident with LN occupation, B cell maturation, and Ig production. B cell production was not sustained over time, potentially due to an insufficient stem cell niche in the mouse or engraftment of non-pluripotent, self-renewing HSCs (11, 15, 28).

Despite several previous studies describing the presence of only immature B cells in hu-mice (14–16), we report here that mature B cells develop in our model. Our observation of mature B cells is likely due to the timing of our experiments (we observe mature B cells in older mice), and the analysis of B cells in LNs, in which we always observe a dominant mature B cell population regardless of age. The analysis of multiple cell surface proteins demonstrates that the phenotype of mature B cells in our hu-mice is quite similar to that of B cells in human blood and tissue (Table I). This is true for markers of maturation, activation, and those related to cellular interaction or trafficking, with few exceptions. We also found that expression of CD44 on B cells of hu-mice is consistent with that of human B cell populations and clearly distinguishes mature B cells (high CD44) from immature B cells (low CD44) (29). Based on a previous study, we cannot exclude the possibility that the mature B cell population in our hu-mice include a late transitional T3 population that is phenotypically indistinguishable from mature naïve B cells by conventional markers (30). However, the fact that some B cells in our hu-mice class-switch to IgG and upregulate activation markers highlights the fact that these cells are functional and suggest that they do not possess an inherent maturation block. Although most of the differentiation markers analyzed showed normal expression levels on mature B cells of hu-mice, there was one notable exception. The expression of CD268 (BAFFR) was significantly reduced compared to that on B cells from human tissues (Table I). We suggest that CD268 might be downregulated in hu-mice following binding to mouse BAFF, which is at super-physiological concentrations relative to B cell numbers (31, 32). A similar phenomenon has been observed in human CB transplantation recipients (33).

In addition to characterizing human hematopoietic engraftment in hu-mice, we also used the model to study human B cell biology. The most notable aspect of this study was our unexpected finding that human T cells provide the resources for human B cell maturation. Our data predicts that in patients and mice with T cell immunodeficiencies, the B cells might have a developmental defect. In fact, the few studies that addressed this issue in humans concluded that B cells in patients with SCID (34), X-linked lymphoproliferative disease, and common-variable immunodeficiency disease (18) are prevalently immature, as they are most similar to the B cells in CB than to those in adult peripheral blood. Another study of patients

with IL7Rα deficiency, a defect that leads to low T cell and normal B cell numbers, observed barely detectable levels of sera Ig, thus suggesting for the presence of immature and/or non-functional B cells (35). Importantly, the delayed T cell reconstitution and its association with impaired B cell function is common, and quite problematic, in the clinical CB transplantation setting (33). A recent finding that CB transplantation in the absence of T cell depletion rapidly recovers the B cell function is consistent with our data that T cells facilitate B cell maturation (21). Because most of the known T cell-specific genetic defects in mice (e.g. TCRαβ$^{-/-}$) and humans (e.g., DiGeorge) do not completely abolish T cell generation, validating our observation and defining the mechanism of T cell-dependent B cell maturation will require future investigation with proper experimental models (e.g., TCRαβ$^{-/-}$γδ$^{-/-}$ mice and manipulated hu-mice).

We found that T cells expressing CD45RO, HLA-DR, CD49d, and CD95 (Fig. 3C and data not shown) were elevated in LNs and in spleens with mature B cells. Upregulation of these markers indicate an activated state, and suggest that the activation of T cells might be required for B cell maturation. Whether the T cells developed de novo in hu-mice from HSC or were transferred exogenously, the correlation of activated T cells with mature B cells in the spleens was consistent. The analysis of CD49d expression, a molecule which has been shown to be upregulated on Ag-activated, but not lymphopenia-activated T cells in mice (36), suggest that both forms of activation occur in hu-mice, as approximately 50% of the CD45RO^{+} T cells in spleen and LNs expressed CD49d. A similar activated phenotype was also observed on CB T cells recovered from BALB/c-DKO mice 3 wks after their adoptive transfer (data not shown), suggesting that T cell activation might also be mediated by reaction with xeno-Ags. Because hu-mice will always provide a lymphopenic and xenogeneic environment that drives T cell activation (37), it will be difficult to discriminate whether activation is required or not for B cell maturation. The activated state of T cells that correlated with B cell maturation was also associated with higher T cell numbers, and T cell numbers strongly correlated with mature B cells. Therefore, it is possible that T cell activation merely expands the T cell population to a size required to drive B cell maturation.

Similarly, our studies do not distinguish whether a CD4 or CD8 T cell subset is responsible for the B cell maturation. We did not observe a correlation between frequencies of CD4 T cells (and conversely of CD8 T cells) and mature B cells in the spleen in both intact hu-mice (Fig. 3C) and in those boosted with CB T cells (data not shown). Preliminary experiments to discern whether CD4 or CD8 subsets are required for the B cell maturation were inconclusive because 3 wks after the injection of highly-purified CD4 or CD8 T cells, a mixed (injected and endogenous CD4 and CD8) T cell population was observed in tissues (data not shown). Notably, the presence of mature B cells in the spleens of these hu-mice correlated with the frequency and number of total T cells, and not with a T cell subset, similar to what we observed in intact hu-mice.

The hu-mouse model is conceptually a very powerful resource for studies of the human hematopoietic system. However, the limitation of inadequate cellular development in these mice still warrants considerable skepticism regarding its usefulness. In this regard, what some may view as a limitation, others may consider a unique resource. An underappreciated advantage of the hu-mouse model is its utility in mapping cellular developmental pathways by adding or removing cellular or molecular components. Using this approach, future studies will explore the specific T cell factors that drive B cell maturation in hu-mice.

Unlike inbred mouse strains, hu-mice are distinct both in their genetics (i.e., the source of HSCs) and engraftment phenotype. In this study, we categorized these phenotypes into 5 classes, based on human engraftment in LNs and the maturation state of B cells in the spleen. We show that the human chimerism of hu-mice changes over time, including a

decline in BM B cell output, and an increase in the engraftment of LNs, the proportion of mature B cells, the production of hIgM and hIgG and the thymic output and expansion of T cells. However, the specific timing of hematopoietic cell reconstitution in individual mice may vary by several wks. For instance, in some hu-mice mature B cells are seen prior to 15 wks, while in others they appear later than 20 wks, and in some they never develop. The best indicator for the presence of mature B cells is not age but rather the frequency of T cells, which can be easily determined by PBL analysis.

The interpretation of Ag-specific ELISA data in hu-mice proved quite challenging. Unlike mice and humans, the sera of hu-mice contain vastly differing Ig concentrations from animal to animal, and in the same animal over time, making it difficult to compare Ab responses in sera of immunized mice relative to pre-immune sera (14, 16, 19, 22), or without proper controls (10, 17). Any hu-mouse sera, whether Ag-reactive or not, generated a background signal that was dependent on the Ig concentration. This background was independent of Ag on the plate, it was present whether the plate was blocked or not with a variety of reagents, and it was absent only in sera of mice that did not contain any Ig. In addition, we observed inherent polyreactivity, particularly in the IgM responses, and similar to polyreactive responses detected both in mice (38) and humans (39, 40), which also increased with Ig concentration. These issues emphasize the need of a well-controlled, standardized Ag-specific Ab assay to allow comparisons among laboratories using hu-mice.

Nonetheless, using our optimized ELISA protocol we were able to determine that immunizing hu-mice later (>14 wks), when T cells and consequently mature B cells reach significant numbers, results in improved Ag-specific responses. Even when hu-mice are immunized early, the Ab response to TD Ag is better in hu-mice with mature B cells in the spleen. These observations suggest that mature B cells support improved Ab responses to immunization in hu-mice. This Ag-specific IgG is particularly relevant in the context of a TD response as it suggests the presence of both a population of competent B cells capable of Ig class-switch and a productive cognate B-T cell collaboration. Our histological studies noted an increased co-localization of human T and B cells in the spleen of mice with mature B cells (9, 26), suggesting the possibility of increased T-B cell cognate interactions. However, these analyses still indicate the presence of an abnormal lymphoid architecture even in those hu-mice with T cells and mature B cells, suggesting that the human cells do not correctly sense the chemokines driving lymphocyte localization. Other studies have shown that supplying a human MHC class II allele to hu-mice (41) or co-transplanting a human thymus (42) enhances T cell-dependent Ab responses. It will be of interest to test whether these responses are further improved in the presence of mature B cells.

The large majority of B cells in all LNs analyzed in hu-mice were mature, clearly differentiating this tissue environment from those of the PBL and spleen. The LNs of hu-mice displayed other unique features: 1) LN anlagen appear to exist in the absence of hematopoietic chimerism (i.e., in intact BALB/c-DKO mice) as suggested by the existence of barely visible structures, and the rapid infiltration of cells following human PBMC injection (data not shown); 2) mouse hematopoietic cells are not detected by flow cytometry within LNs in the absence of human hematopoietic cells; 3) only a subset of hu-mice harbor engrafted LNs – the engraftment appears to depend on time, absolute chimerism, and presence of T cells; 4) human hematopoietic engraftment of LNs is greatly delayed (> 2 months) compared to human engraftment of BM, spleen and PBL; 5) LNs are differentially engrafted – mesenteric LNs are populated earlier and more commonly than peripheral LNs; however, even hematopoietic engraftment of peripheral LNs, which occurs typically in mice with dominant T cell chimerism, is irregular, with cervical and axillary LN engraftment more common but inconsistent and often unilateral; 6) the LNs contain a fraction of CD4/CD8 double-positive T cells (data not shown) that is normally found only in the thymus; and

7) the ratio of human T:B cells in the LNs is highly consistent and physiological (2:1) compared to the spleen. Our data overall suggest that the high frequency of mature B cells in the LN is due to the high proportion of T cells in this organ. The presence of a minor population of immature B cells in the LN suggests that B cell maturation takes place within this tissue after entry and that it is not a requirement for entry into the LN.

The engraftment dynamics of LNs in hu-mice can potentially provide clues for understanding the mechanisms of murine and human LN development. We noticed that the spleen and BM of hu-mice with engrafted LNs display a correlative increase of human $CD4^+CD3^-CD20^-$ cell numbers (data not shown). Cells with this phenotype have been implicated in the seeding of LNs in mice (43, 44), suggesting that they might be also promoting LN occupation in hu-mice. Alternatively, T cells might develop extrathymically directly in the LN, a phenomenon that is amplified by oncostatin M (OM) and that is frequently observed in OM transgenic mice and, at times, in athymic mice (45). T cell development also occurs in the LNs of wildtype mice, although this process is inhibited or out-competed by thymic-derived T cells (45). T cells in the LNs of hu-mice display a hyper-proliferative and a hyper-apoptotic phenotype (Fig. 3C and data not shown), which is consistent with T cells in LNs of OM Tg mice. In addition, the more frequent development of mesenteric LNs over axillary and cervical LNs in hu-mice is similar to that observed in OM Tg mice (45). Thus, whether the LNs in hu-mice are engrafted by specific $CD4^+CD3^-$ precursors or are the site of extrathymic T cell development remains to be determined. The inconsistent frequency and site of LN engraftment among hu-mice suggests this is a relatively rare, stochastic event.

A final point of this study is the reliability of the BALB/c-DKO hu-mouse model as an experimental model of the human immune system. We believe that this model transplanted with CB HSCs offers certain advantages, including consistent engraftment of HSCs, longevity, productive breeding, significant thymic engraftment and T cell generation without the need of human thymus co-transplantation (16, 46), and robust IgG production. Furthermore, the susceptibility of the BALB/c embryonic stem cells to genetic manipulation makes it easier to introduce novel mutations. In this regard, other investigators have generated novel BALB/c-DKO strains that express human genes designed to enhance human hematopoietic engraftment, survival and differentiation (47, 48).

Using this model, we were able to analyze human hematopoietic cells in hu-mice for longer than four months and detect mature B cells. This is an important finding considering the numerous reports of a B cell maturation block in hu-mice. We also determined that the generation of mature, naïve B cells in hu-mice is dependent on the presence of human T cells. Notably, this B cell population is functional and produces improved Ag-specific T-independent and T-dependent Ab responses over those measured in hu-mice with immature B cells. This suggests that experimental vaccine studies in hu-mice should be performed in older mice with higher frequencies of mature B cells, which can be estimated by the frequency of PBL T cells. Thus, this study enhances both the usefulness of the hu-mouse model and our understanding of human B cell development.

Supplementary Material

Refer to Web version on PubMed Central for supplementary material.

Acknowledgments

The authors would like to acknowledge Josh Loomis in the flow cytometry core at National Jewish Health for technical help, Nick Weiss for technical assistance, Kim Jordan for providing human spleen cells, and Katie Haskins (UCD, NJH) and Lenka Teodorovic (UCD, NJH) for critical reading of the manuscript.

This work was supported by the National Institute of Health with the R21-AI073629 grant (RP), the Arthritis Foundation with an Innovative Research Grant (RP), a NJH Translational Research Initiative grant (RP), and Department of Defense grant W81AWH-07-01-0550 (RK).

References

1. Traggiai E, Chicha L, Mazzucchelli L, Bronz L, Piffaretti JC, Lanzavecchia A, Manz MG. Development of a human adaptive immune system in cord blood cell-transplanted mice. Science. 2004; 304:104–107. [PubMed: 15064419]
2. Ishikawa F, Yasukawa M, Lyons B, Yoshida S, Miyamoto T, Yoshimoto G, Watanabe T, Akashi K, Shultz LD, Harada M. Development of functional human blood and immune systems in NOD/SCID/IL2 receptor {gamma} chain(null) mice. Blood. 2005; 106:1565–1573. [PubMed: 15920010]
3. Gimeno R, Weijer K, Voordouw A, Uittenbogaart CH, Legrand N, Alves NL, Wijnands E, Blom B, Spits H. Monitoring the effect of gene silencing by RNA interference in human CD34+ cells injected into newborn RAG2−/− gammac−/− mice: functional inactivation of p53 in developing T cells. Blood. 2004; 104:3886–3893. [PubMed: 15319293]
4. Ito M, Hiramatsu H, Kobayashi K, Suzue K, Kawahata M, Hioki K, Ueyama Y, Koyanagi Y, Sugamura K, Tsuji K, Heike T, Nakahata T. NOD/SCID/gamma(c)(null) mouse: an excellent recipient mouse model for engraftment of human cells. Blood. 2002; 100:3175–3182. [PubMed: 12384415]
5. Hiramatsu H, Nishikomori R, Heike T, Ito M, Kobayashi K, Katamura K, Nakahata T. Complete reconstitution of human lymphocytes from cord blood CD34+ cells using the NOD/SCID/gammacnull mice model. Blood. 2003; 102:873–880. [PubMed: 12689924]
6. Akkina R, Berges BK, Palmer BE, Remling L, Neff CP, Kuruvilla J, Connick E, Folkvord J, Gagliardi K, Kassu A, Akkina SR. Humanized Rag1−/− gammac−/− mice support multilineage hematopoiesis and are susceptible to HIV-1 infection via systemic and vaginal routes. PLoS One. 2011; 6:e20169. [PubMed: 21695116]
7. Tanaka S, Saito Y, Kunisawa J, Kurashima Y, Wake T, Suzuki N, Shultz LD, Kiyono H, Ishikawa F. Development of mature and functional human myeloid subsets in hematopoietic stem cell-engrafted NOD/SCID/IL2rgammaKO mice. J Immunol. 2012; 188:6145–6155. [PubMed: 22611244]
8. Pearson T, Shultz LD, Miller D, King M, Laning J, Fodor W, Cuthbert A, Burzenski L, Gott B, Lyons B, Foreman O, Rossini AA, Greiner DL. Non-obese diabetic-recombination activating gene-1 (NOD-Rag1 null) interleukin (IL)-2 receptor common gamma chain (IL2r gamma null) null mice: a radioresistant model for human lymphohaematopoietic engraftment. Clin Exp Immunol. 2008; 154:270–284. [PubMed: 18785974]
9. Gorantla S, Sneller H, Walters L, Sharp JG, Pirruccello SJ, West JT, Wood C, Dewhurst S, Gendelman HE, Poluektova L. Human immunodeficiency virus type 1 pathobiology studied in humanized BALB/c-Rag2−/−gammac−/− mice. J Virol. 2007; 81:2700–2712. [PubMed: 17182671]
10. Choi B, Chun E, Kim M, Kim ST, Yoon K, Lee KY, Kim SJ. Human B cell development and antibody production in humanized NOD/SCID/IL-2Rgamma(null) (NSG) mice conditioned by busulfan. J Clin Immunol. 2011; 31:253–264. [PubMed: 20981478]
11. Shultz LD, Ishikawa F, Greiner DL. Humanized mice in translational biomedical research. Nat Rev Immunol. 2007; 7:118–130. [PubMed: 17259968]
12. Ito R, Takahashi T, Katano I, Ito M. Current advances in humanized mouse models. Cell Mol Immunol. 2012; 9:208–214. [PubMed: 22327211]
13. Manz MG, Di Santo JP. Renaissance for mouse models of human hematopoiesis and immunobiology. Nat Immunol. 2009; 10:1039–1042. [PubMed: 19767720]
14. Watanabe Y, Takahashi T, Okajima A, Shiokawa M, Ishii N, Katano I, Ito R, Ito M, Minegishi M, Minegishi N, Tsuchiya S, Sugamura K. The analysis of the functions of human B and T cells in humanized NOD/shiscid/gammac(null) (NOG) mice (hu-HSC NOG mice). Int Immunol. 2009; 21:843–858. [PubMed: 19515798]
15. Vuyyuru R, Patton J, Manser T. Human immune system mice: current potential and limitations for translational research on human antibody responses. Immunol Res. 2011; 51:257–266. [PubMed: 22038527]

16. Biswas S, Chang H, Sarkis PT, Fikrig E, Zhu Q, Marasco WA. Humoral immune responses in humanized BLT mice immunized with West Nile virus and HIV-1 envelope proteins are largely mediated via human CD5+ B cells. Immunology. 2011; 134:419–433. [PubMed: 22044090]

17. Matsumura T, Kametani Y, Ando K, Hirano Y, Katano I, Ito R, Shiina M, Tsukamoto H, Saito Y, Tokuda Y, Kato S, Ito M, Motoyoshi K, Habu S. Functional CD5+ B cells develop predominantly in the spleen of NOD/SCID/gammac(null) (NOG) mice transplanted either with human umbilical cord blood, bone marrow, or mobilized peripheral blood CD34+ cells. Exp Hematol. 2003; 31:789–797. [PubMed: 12962725]

18. Cuss AK, Avery DT, Cannons JL, Yu LJ, Nichols KE, Shaw PJ, Tangye SG. Expansion of functionally immature transitional B cells is associated with human-immunodeficient states characterized by impaired humoral immunity. J Immunol. 2006; 176:1506–1516. [PubMed: 16424179]

19. Baenziger S, Tussiwand R, Schlaepfer E, Mazzucchelli L, Heikenwalder M, Kurrer MO, Behnke S, Frey J, Oxenius A, Joller H, Aguzzi A, Manz MG, Speck RF. Disseminated and sustained HIV infection in CD34+ cord blood cell-transplanted Rag2−/−gamma c−/− mice. Proc Natl Acad Sci U S A. 2006; 103:15951–15956. [PubMed: 17038503]

20. Garcia S, Freitas AA. Humanized mice: Current states and perspectives. Immunol Lett. 2012; 146:1–7. [PubMed: 22507217]

21. Chiesa R, Gilmour K, Qasim W, Adams S, Worth AJ, Zhan H, Montiel-Equihua CA, Derniame S, Cale C, Rao K, Hiwarkar P, Hough R, Saudemont A, Fahrenkrog CS, Goulden N, Amrolia PJ, Veys P. Omission of in vivo T-cell depletion promotes rapid expansion of naive CD4+ cord blood lymphocytes and restores adaptive immunity within 2 months after unrelated cord blood transplant. Br J Haematol. 2012; 156:656–666. [PubMed: 22224700]

22. Lepus CM, Gibson TF, Gerber SA, Kawikova I, Szczepanik M, Hossain J, Ablamunits V, Kirkiles-Smith N, Herold KC, Donis RO, Bothwell AL, Pober JS, Harding MJ. Comparison of human fetal liver, umbilical cord blood, adult blood hematopoietic stem cell engraftment in NOD-scid/gammac −/−, Balb/c-Rag1−/−gammac−/−, C.B-17-scid/bg immunodeficient mice. Hum Immunol. 2009; 70:790–802. [PubMed: 19524633]

23. Lang J, Weiss N, Freed BM, Torres RM, Pelanda R. Generation of hematopoietic humanized mice in the newborn BALB/c-Rag2null Il2rgammanull mouse model: a multivariable optimization approach. Clin Immunol. 2011; 140:102–116. [PubMed: 21536497]

24. Imamura M, Tsutsumi Y, Miura Y, Toubai T, Tanaka J. Immune reconstitution and tolerance after allogeneic hematopoietic stem cell transplantation. Hematology. 2003; 8:19–26. [PubMed: 12623423]

25. Williams KM, Gress RE. Immune reconstitution and implications for immunotherapy following haematopoietic stem cell transplantation. Best Pract Res Clin Haematol. 2008; 21:579–596. [PubMed: 18790456]

26. Watanabe S, Ohta S, Yajima M, Terashima K, Ito M, Mugishima H, Fujiwara S, Shimizu K, Honda M, Shimizu N, Yamamoto N. Humanized NOD/SCID/IL2Rgamma(null) mice transplanted with hematopoietic stem cells under nonmyeloablative conditions show prolonged life spans and allow detailed analysis of human immunodeficiency virus type 1 pathogenesis. J Virol. 2007; 81:13259–13264. [PubMed: 17881441]

27. van Krieken JH, te Velde J. Normal histology of the human spleen. Am J Surg Pathol. 1988; 12:777–785. [PubMed: 3421415]

28. Pearson T, Greiner DL, Shultz LD. Humanized SCID mouse models for biomedical research. Curr Top Microbiol Immunol. 2008; 324:25–51. [PubMed: 18481451]

29. Sims GP, Ettinger R, Shirota Y, Yarboro CH, Illei GG, Lipsky PE. Identification and characterization of circulating human transitional B cells. Blood. 2005; 105:4390–4398. [PubMed: 15701725]

30. Palanichamy A, Barnard J, Zheng B, Owen T, Quach T, Wei C, Looney RJ, Sanz I, Anolik JH. Novel human transitional B cell populations revealed by B cell depletion therapy. J Immunol. 2009; 182:5982–5993. [PubMed: 19414749]

31. Schmidt MR, Appel MC, Giassi LJ, Greiner DL, Shultz LD, Woodland RT. Human BLyS facilitates engraftment of human PBL derived B cells in immunodeficient mice. PLoS One. 2008; 3:e3192. [PubMed: 18784835]

32. Kreuzaler M, Rauch M, Salzer U, Birmelin J, Rizzi M, Grimbacher B, Plebani A, Lougaris V, Quinti I, Thon V, Litzman J, Schlesier M, Warnatz K, Thiel J, Rolink AG, Eibel H. Soluble BAFF levels inversely correlate with peripheral B cell numbers and the expression of BAFF receptors. J Immunol. 2011; 188:497–503. [PubMed: 22124120]
33. Bunin N, Small T, Szabolcs P, Baker KS, Pulsipher MA, Torgerson T. NCI, NHLBI/PBMTC first international conference on late effects after pediatric hematopoietic cell transplantation: persistent immune deficiency in pediatric transplant survivors. Biol Blood Marrow Transplant. 2012; 18:6–15. [PubMed: 22100979]
34. Small TN, Keever C, Collins N, Dupont B, O'Reilly RJ, Flomenberg N. Characterization of B cells in severe combined immunodeficiency disease. Hum Immunol. 1989; 25:181–193. [PubMed: 2670851]
35. Roifman CM, Zhang J, Chitayat D, Sharfe N. A partial deficiency of interleukin-7R alpha is sufficient to abrogate T-cell development and cause severe combined immunodeficiency. Blood. 2000; 96:2803–2807. [PubMed: 11023514]
36. Haluszczak C, Akue AD, Hamilton SE, Johnson LD, Pujanauski L, Teodorovic L, Jameson SC, Kedl RM. The antigen-specific CD8+ T cell repertoire in unimmunized mice includes memory phenotype cells bearing markers of homeostatic expansion. J Exp Med. 2009; 206:435–448. [PubMed: 19188498]
37. Onoe T, Kalscheuer H, Chittenden M, Zhao G, Yang YG, Sykes M. Homeostatic expansion and phenotypic conversion of human T cells depend on peripheral interactions with APCs. J Immunol. 2010; 184:6756–6765. [PubMed: 20483739]
38. Lymberi P, Blancher A, Calvas P, Avrameas S. Natural autoantibodies in nude and normal outbred (Swiss) and inbred (BALB/c) mice. J Autoimmun. 1989; 2:283–295. [PubMed: 2765099]
39. Amlot PL, Hayes AE. Impaired human antibody response to the thymus-independent antigen, DNP-Ficoll, after splenectomy. Implications for post-splenectomy infections. Lancet. 1985; 1:1008–1011. [PubMed: 2859463]
40. Amlot PL, Hayes AE, Gray D, Gordon-Smith EC, Humphrey JH. Human immune responses in vivo to protein (KLH) and polysaccharide (DNP-Ficoll) neoantigens: normal subjects compared with bone marrow transplant patients on cyclosporine. Clin Exp Immunol. 1986; 64:125–135. [PubMed: 2426019]
41. Danner R, Chaudhari SN, Rosenberger J, Surls J, Richie TL, Brumeanu TD, Casares S. Expression of HLA class II molecules in humanized NOD.Rag1KO.IL2RgcKO mice is critical for development and function of human T and B cells. PLoS One. 2011; 6:e19826. [PubMed: 21611197]
42. Tonomura N, Habiro K, Shimizu A, Sykes M, Yang YG. Antigen-specific human T-cell responses and T cell-dependent production of human antibodies in a humanized mouse model. Blood. 2008; 111:4293–4296. [PubMed: 18270327]
43. Lane PJ, Gaspal FM, Kim MY. Two sides of a cellular coin: CD4(+)CD3- cells regulate memory responses and lymph-node organization. Nat Rev Immunol. 2005; 5:655–660. [PubMed: 16034364]
44. Cupedo T, Kraal G, Mebius RE. The role of CD45+CD4+CD3-cells in lymphoid organ development. Immunol Rev. 2002; 189:41–50. [PubMed: 12445264]
45. Blais ME, Louis I, Perreault C. T-cell development: an extrathymic perspective. Immunol Rev. 2006; 209:103–114. [PubMed: 16448537]
46. Kalscheuer H, Danzl N, Onoe T, Faust T, Winchester R, Goland R, Greenberg E, Spitzer TR, Savage DG, Tahara H, Choi G, Yang YG, Sykes M. A model for personalized in vivo analysis of human immune responsiveness. Sci Transl Med. 2012; 4 125ra130.
47. Willinger T, Rongvaux A, Strowig T, Manz MG, Flavell RA. Improving human hemato-lymphoid-system mice by cytokine knock-in gene replacement. Trends Immunol. 2011; 32:321–327. [PubMed: 21697012]
48. Strowig T, Rongvaux A, Rathinam C, Takizawa H, Borsotti C, Philbrick W, Eynon EE, Manz MG, Flavell RA. Transgenic expression of human signal regulatory protein alpha in Rag2−/−gamma(c)−/− mice improves engraftment of human hematopoietic cells in humanized mice. Proc Natl Acad Sci U S A. 2011; 108:13218–13223. [PubMed: 21788509]

Abbreviations used in this article

AP	alkaline phosphatase
BALB/c-DKO	BALB/c-Rag2^{null}Il2rγ^{null}
BM	bone marrow
CB	cord blood
DTaP	Diptheria, Tetanus, and Pertussis
DT	Diptheria Toxin
HSC	hematopoietic stem cell
hu-mouse	humanized mouse
LN	lymph node
NJH	National Jewish Health
PBL	peripheral blood
TD	T-dependent
TI	T-independent
UCD	University of Colorado Denver

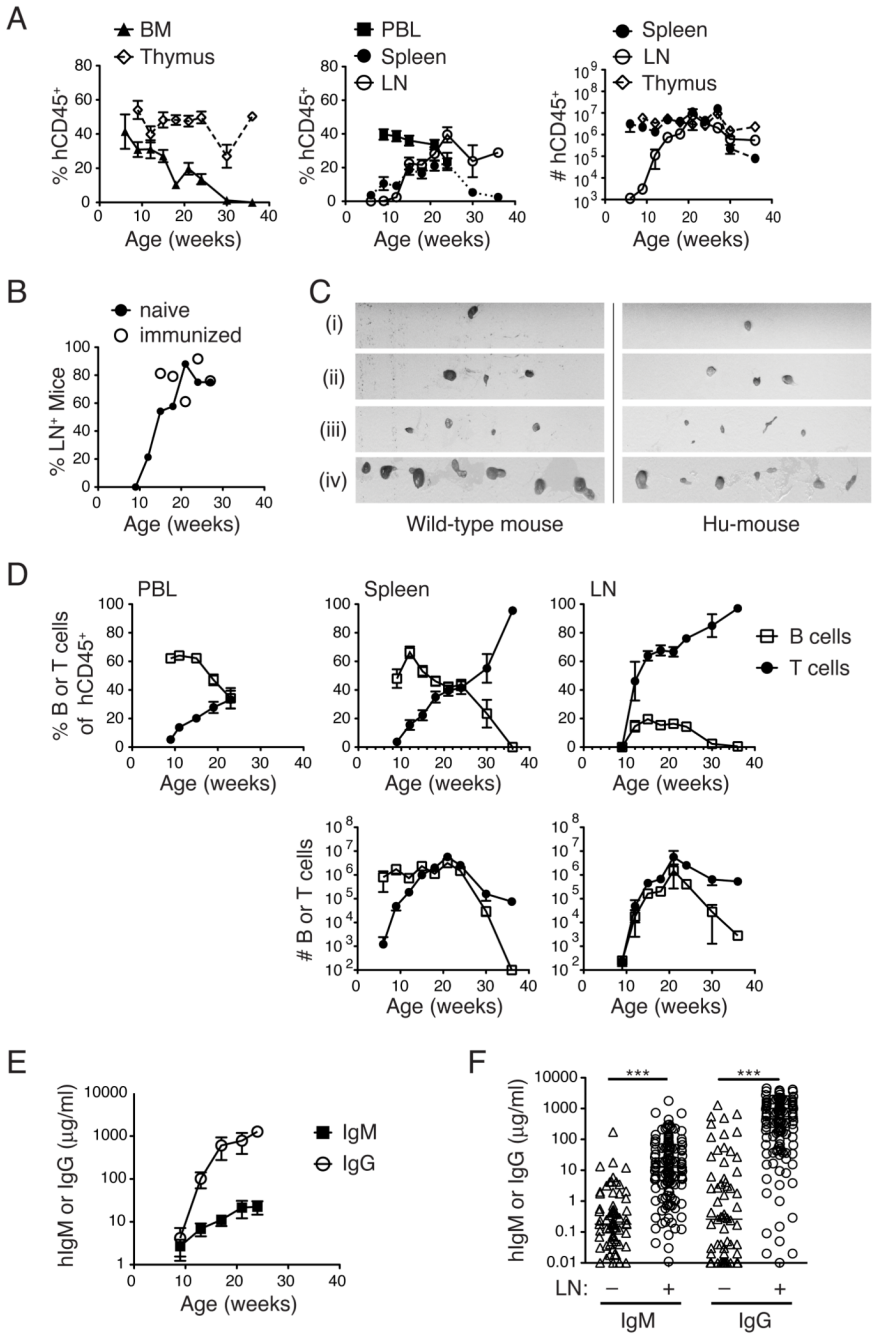

FIGURE 1.

Kinetics of human hematopoietic cell engraftment in BALB/c-DKO hu-mice. (A) Humanized BALB/c-DKO mice were analyzed for human chimerism in the PBL at 3–4 wk intervals beginning at 7–8 wks of age, and in the BM, thymus, spleen and LN upon harvest. The animals were euthanized at indicated ages (n = 4–51 for 6–30 wks, and n = 1 for 37 wks). Human chimerism was determined by FACS analysis of cells stained with anti-human and anti-mouse CD45 Abs. In the BM, PBL and spleen, the percentage of human $CD45^+$ cells is calculated relative to total (mouse + human) hematopoietic cells, whereas in the LN and thymus the percentage of $hCD45^+$ cells is reported in the total live cell gate. The absolute cell numbers of $hCD45^+$ cells in LN, thymus and spleen of hu-mice at different

time points are shown in the right panel. Graphs show the mean ± SEM. (B) Frequency of hu-mice at indicated age in wks displaying detectable LNs (mesenteric, axillary, inguinal, cervical or iliac), as defined by tissue exhibiting >1% $hCD45^+$ cells by FACS analysis. Open symbols indicate hu-mice that were immunized as described in Fig. 4. (C) Iliac (i), cervical (ii), inguinal and axillary (iii), and mesenteric (iv) LNs were excised from a control CB17 mouse (left panels) and a 24 wk-old hu-mouse (right panels). All images shown are from the same photograph and, therefore, on equivalent scale. (D) Top panels: the percentage of $CD20^+$ B cells (open square) and $CD3^+CD5^+$ T cells (closed circle) within the $hCD45^+$ gate in the PBL (left), spleen (middle) and LNs (right) of hu-mice at indicated ages. Bottom panels: the absolute number of human B and T cells in the spleen (middle) and LNs (right). Data represent the mean ± SEM (n =1 at 37 wks and n =4–52 for all other points). (E) Human IgM and IgG concentrations (μg/ml) in the sera of hu-mice (n = 17) at indicated age. Data are mean ± SEM. (F) Human IgM and IgG concentration in sera of hu-mice that either harbor (n = 125–131) or not (n = 67–71) LNs at time of euthanasia. Each symbol represents an individual mouse and horizontal bars the median. (***p<0.001)

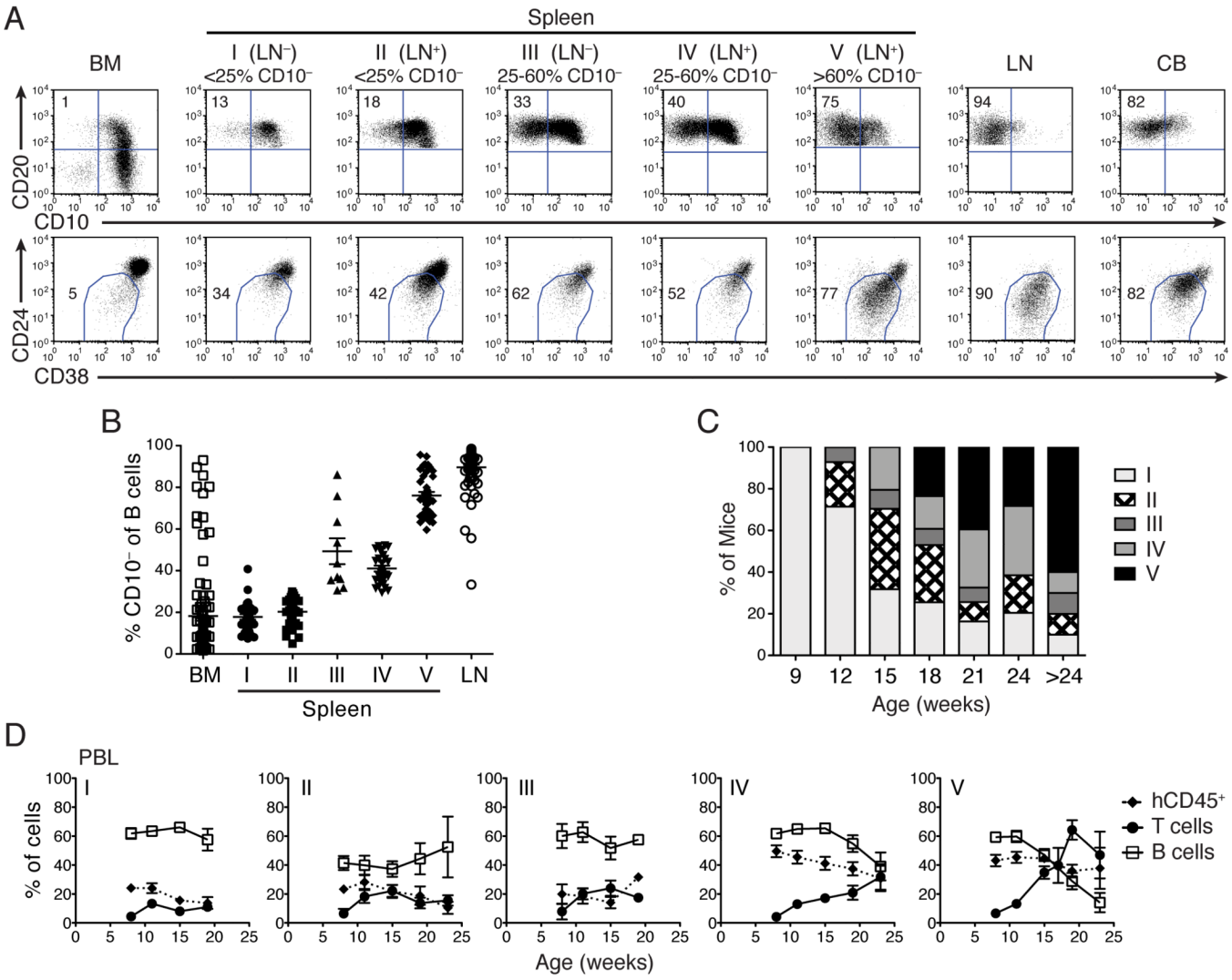

FIGURE 2.

Hu-mice categorization based on B cell maturation and LN engraftment. (A) Maturation of B cells in the BM, spleen, and LN of representative hu-mice and in a human CB sample as determined by expression of CD10 (top row), or CD24 and CD38 (bottom row) on B cells gated as $CD19^+$ (BM) or $CD20^+$ (spleen, LN, and CB). Numbers represent the frequency of $CD10^-$ (top) and $CD24^{low}CD38^{low}$ (bottom) mature B cells in the gate. Hu-mice were classified in 5 categories (I–V) according to the presence of LNs and the frequency of mature B cells in the spleen: I) LN^-, <25% $CD10^-$; II) LN^+, <25% $CD10^-$; III) LN^-, >25% $CD10^-$; IV) LN^+, 25–60% $CD10^-$; and V) LN+, >60% $CD10^-$. (B) Percentage of mature $CD10^-$ B cells in BM, spleen and LN of individual hu-mice (n = 142) grouped according to the categories described in (A). (C) The frequencies of hu-mice classified in the five categories (I–V) described in (A) at 9, 12, 15, 18, 21, 24 and >24 wks of age (n = 10–51 per age). (D) Frequencies of human hematopoietic cells ($hCD45^+$, closed diamond), T cells ($CD3^+CD5^+$, closed circle) and B cells ($CD20^+$, open square) in PBL of hu-mice assigned to the five categories described in (A) and at indicated ages. The frequency of $hCD45^+$ cells was measured in the total (mouse + human) $CD45^+$ cell population. The frequencies of B and T cells were measured within the $hCD45^+$ cell gate. Data represent the mean ± SEM (n

= 5–38 mice per time point and category, besides category II at 23w (n =2) and category III at 19w (n =1)).

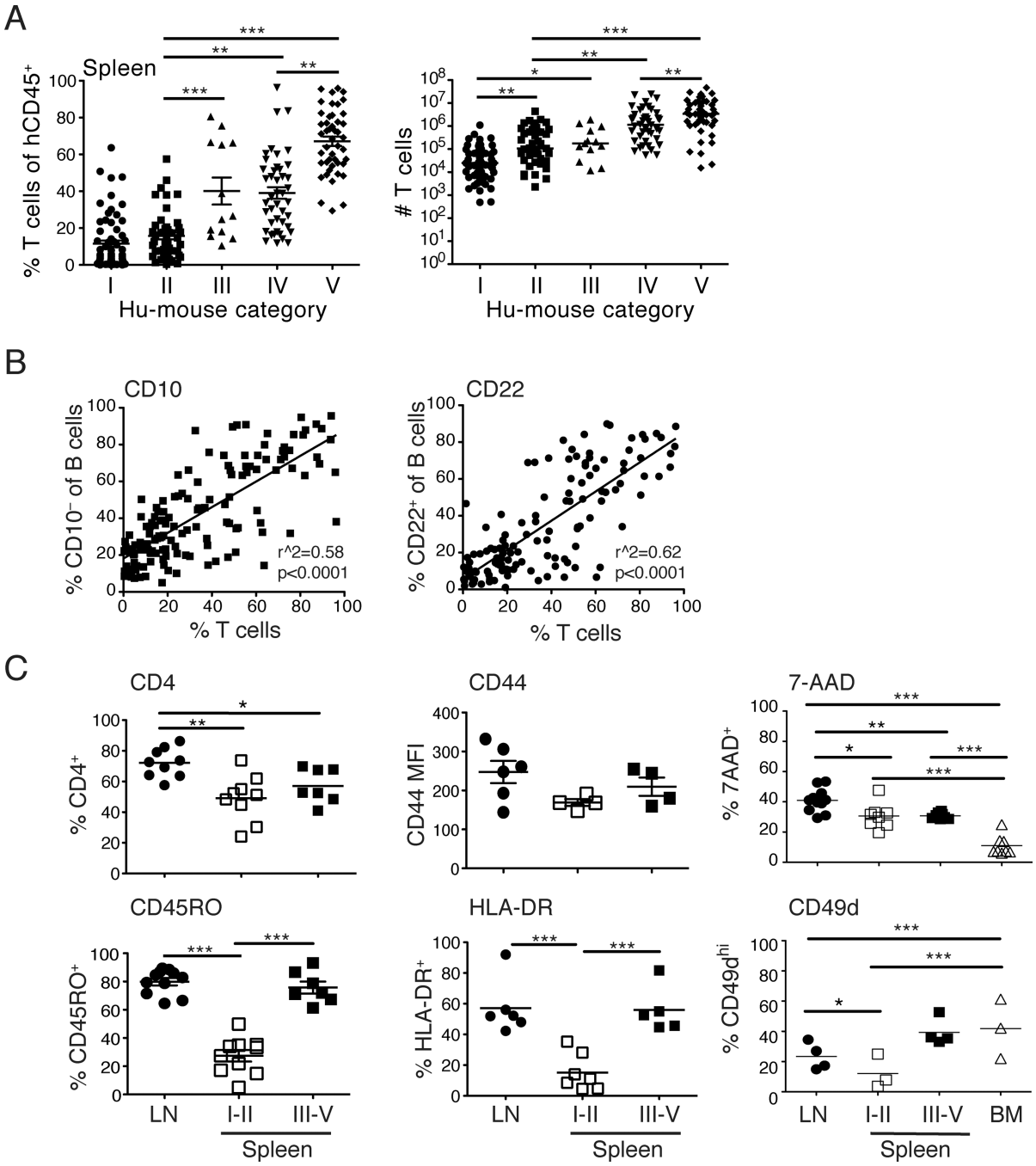

FIGURE 3.

Characterization of T cells in hu-mice. (A) The percentage (left panel) and number (right panel) of ($CD3^+CD5^+$) T cells in the spleen of hu-mice classified according to the five categories described in Fig. 2A at time of euthanasia. Each symbol represents an individual mouse and bars represent mean ± SEM in left panel and median in right panel. (*p<0.05, **p<0.01, ***p<0.001) (B) Linear regression analysis of the percentage of mature B cells ($CD10^−$, left panel and $CD22^+$, right panel) relative to the percentage of T cells in the spleen of individual hu-mice (n = 127–144). Each symbol represents an individual mouse. (C) Analysis of T cells in LNs and in spleen from mice of categories I–II and III–V (as described in Fig. 2A). The panels show the percentage of $CD4^+$, $CD45RO^+$, $HLA\text{-}DR^+$, 7-

AAD^+ and $CD49d^+$ cells, and the m.f.i. of CD44 in the $hCD45^+CD3^+$ T cell gate. Symbols represent individual mice and bars the mean ± SEM (n = 4–10). (*p<0.05, **p<0.01, ***p<0.001)

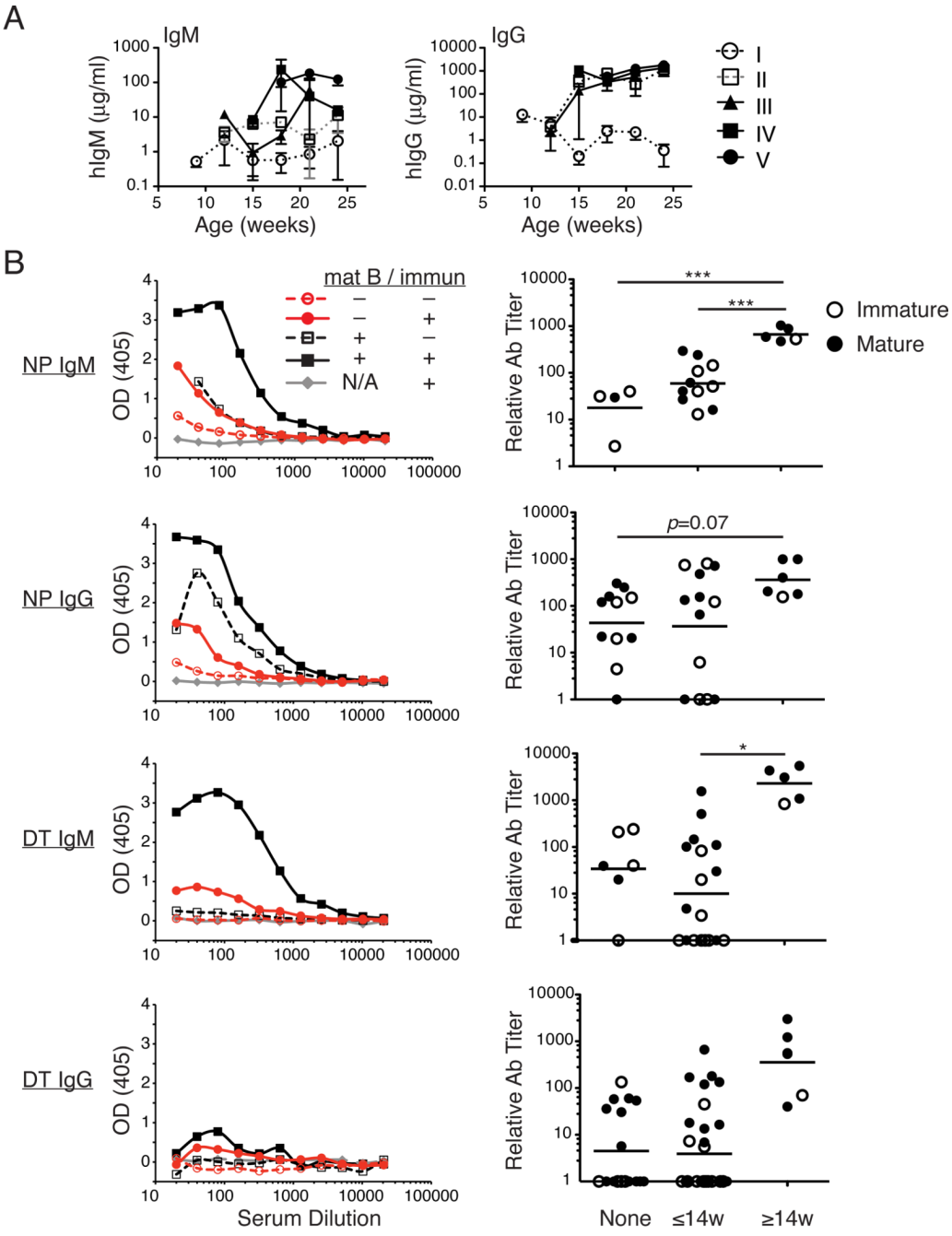

FIGURE 4.

Improved Ab responses to TI and TD immunizations in hu-mice with mature B cells. (A) Concentration (µg/ml) of hIgM (left) and hIgG (right) in sera of hu-mice of categories I–V. The data represent the mean ± SEM of $n = 3–17$ samples per time point and per category with the exception of category III, 12 wks ($n = 1$). (B) Hu-mice were immunized or not with either the TI-II Ag NP-Ficoll (top four panels) or the TD Ag DTaP (bottom four panels) between 8 and 14 (≤14) or 14 and 22 (≥14) wks of age as described in Materials and Methods. Left panels show representative ELISA curves with OD_{405} on the y-axis and sera dilutions on the x-axis. Each graph includes hu-mice that were immunized (intact line, filled symbols) or not (dashed line, empty symbols) and that displayed mostly mature (black lines)

or immature (red lines) B cells, and relative to an immunized intact BALB/c-DKO mouse. The right panels show relative Ab titers (calculated as described in Materials and Methods) in hu-mice that were non-immunized (None), or immunized before (≤14w) or after (≥14w) 14 wks of age, and displaying mature B cells (closed circles) or immature B cells (open circles) in the spleen. (*$p<0.05$, ***$p<0.001$)

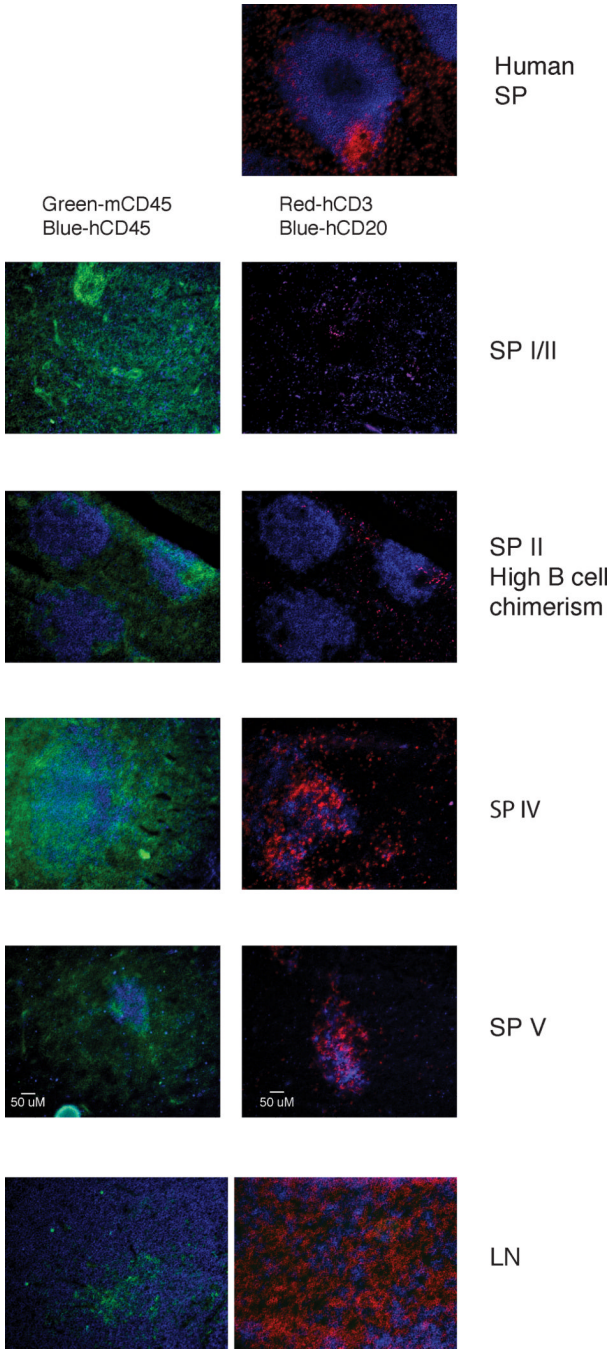

FIGURE 5.

Immunofluorescent histology of LNs and spleens from hu-mice. Tissue sections were stained with Abs against mCD45 (green) and hCD45 (blue) (left panels), or hCD3 (red) and hCD20 (blue) (right panels). Representative sections of a human spleen (top panel), of spleens from hu-mice of categories I, II, IV and V (as described in Fig. 2A), and of LN tissue from a hu-mouse of category IV are shown. Sections shown are 10X magnifications and are representative of at least two samples from a minimum of 3 mice per category, with the exception of category II (high B cell numbers) that represents only one sample. The human spleen section is representative of more than 8 sections from two individuals.

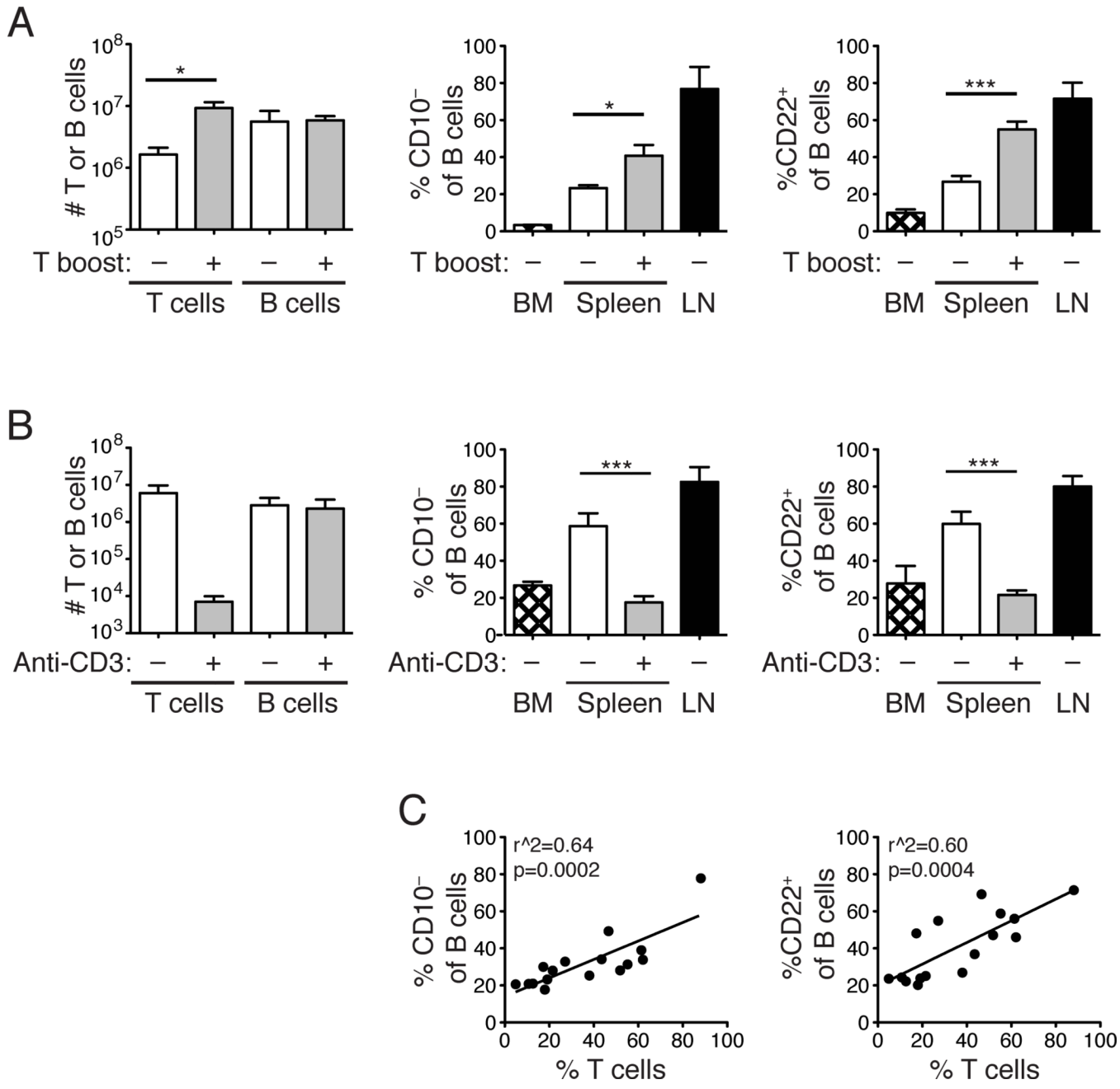

FIGURE 6.

Human T cells are required for B cell maturation. (A) Maturation of B cells in hu-mice adoptively transferred with autologous T cells. Hu-mice were injected (+ T boost) or not (− T boost) at 11–12 wks of age with autologous T cells and harvested at 13–15 wks. Left panel: numbers of T and B cells in the spleens. Middle and right panels: frequencies of mature B cells ($CD10^{-}$, middle panel; $CD22^{+}$ right panel) in the spleens of mice injected or not with T cells. The frequencies of mature B cells in BM and LNs in control untreated hu-mice are shown as reference of tissues with a majority of immature B cells and mature B cells, respectively. Data represent mean ± SEM of 8 cumulative mice per group from three independent experiments. Representative FACS data is shown in Fig. S1A. (B) B cell maturation in hu-mice treated with CD3-depleting Abs. Left panel: numbers of T and B cells

in spleens of hu-mice injected (+) or not (−) semi-weekly with CD3 depleting Abs from 9 wks of age (n = 5–8). Middle and right panels: frequencies of mature B cells ($CD10^-$, middle panel; $CD22^+$ right panel) in the spleens of mice injected or not with anti-CD3 Abs (n = 6–8 per group). The frequencies of mature B cells in BM and LNs in control untreated hu-mice are shown as reference. Data represent mean ± SEM of 6–8 cumulative mice per group from three independent experiments. Representative FACS data is shown in Fig. S1B. (C) Linear regression analysis for mature B cells (CD10, left panel; CD22, right panel) as a function of T cell frequency in the spleen in all mice described in (A). Data are cumulative from three independent experiments. (*p<0.05, ***p<0.001)

Table I

Characterization of B cells in tissues from humans and hu-mice

Marker	Cord Blood	Hu. PBL	Hu. SP	Hu. LN	Hu. BM	Hu-Mo BM CD19$^+$ CD20$^-$	Hu-mo BM CD19$^+$ CD20$^+$	Hu-mo SP I-II	Hu-mo SP III-V	Hu-mo LN
CD19[a]	+++	++++	+++	+++	+++	+++	+++	+++	+++	++
CD20[a]	++++	+++	++	++	+	–	+	+++	+++	++++
CD45RA[a]	++++	++++	+++	++++	++++	+++	+++	+++	++++	++++
CD45[a]	+++	+++	++	++	+++	++	++	++	+++	+++
CD5[b]	+	+/–	+/–	+/–	+/–	–	+	++	++	++
CD10[b]	+	+/–	+/–	–	+++	++++	++++	+++	+(+)	+/–
CD24[a]	+++	++	++	+	++++	++++	++++	+++	++	+
CD38[a]	++	+	+	+	+++	++++	++++	+++	++	+
CD40[a]	++++	++++	++++	++++	+	–	+/–	+	+++	++
HLA-DR[a]	+++	++	++++	+	+++	+++	+++	++	+++	++++
CD21[b]	+++	+++	+++	++	+/–	–	–	–	+	++
CD22[b]	+++	++++	++++	++	+	–	–	+/–	++	+++
CD268[a]	+++	++++	+++	+++	++++	–	+/–	+	+	+
CD23[b]	++	+++	++	+/–	+/–	–	+/–	+/–	++	++
CD27[b]	+/–	++	+++	+++	–	–	–	–	+	++
CD70[b]	+	ND	ND	ND	ND	–	–	–	+/–	++
CD25[b]	–	+/–	–	+	–	–	–	–	–	–
CD69b	–	–	–	–	–	–	–	–	–	–
CD80[b]	–	–	+	–	–	–	–	+	–	–
CD86[b]	+	+	+	+	ND	ND	ND	+	++	++
CD122[b]	+/–	ND	ND	ND	ND	ND	ND	–	ND	+/–
CD11c[b]	+/–	+	+	+	–	–	–	–	++	+++
CD95[b]	–	–	–	–	–	–	–	+/–	++	+++
CD45RB[b]	+	ND	ND	ND	ND	–	+	++	++	++
IgM[a]	++++	+++	++	+	+++	+/–	++++	++++	+++	+++
IgD[a,b]	++++	+++	++	+	++	–	+/–	+	++	++
IgG[b]	+/–	++	++++	+++	ND	–	–	–	+/–	++
CD62L[b]	++	+++	++	+/–	ND	–	–	+/–	+/–	+
CD44[b]	++++	++++	+++	++++	++++	–	+/-	+/–	+++	++++
CD49d[b]	+++	+++	++	++	+++	–	+++	+	+/–	+
LFA-1[a]	++	++	++	++	++	–	+/–	–	++	++
CCR6[a]	+++	+++	–	+/–	–	–	+	++	++	++
CCR7[a]	++	+	ND	ND	ND	–	–	–	+/–	+
CXCR4[a]	+++	+++	++++	++++	+++	–	+	++	++	+++
CXCR5[a]	++	ND	ND	ND	ND	–	+/–	+	–	+++

Analysis of protein expression was performed by flow cytometry on gated human (Hu.) and humouse (Hu-mo.) B cells defined as $hCD45^+$ and $CD19^+$ and/or $CD20^+$. In the bone marrow (BM) of hu-mice, analysis was also performed on the developmental early fraction of $CD19^+CD20^-$ B cells. Analysis of spleen B cells from hu-mice is separated for mice of categories I–II and III–V. The relative protein expression level (a) or frequency of positive cells (b) is depicted in a grayscale format and with + and − symbols, with black and ++++ representing the highest expression (a) or frequency (b). ND = not determined.